



**university of
 groningen**

faculty of science and
 engineering

biomedical
 engineering

Effect of impact energy on the formation of micro-cracks on healthy bovine cartilage

Eleana Kostopoulou
 S5342503

University Medical Center Groningen – Orthopaedics Department

Period: 17/04/2023 - 30/06/2023

Internship

Supervisor: Dr. Hugo van der Veen – Department of Orthopaedics – University
 Medical Center Groningen

Examiners: Dr. Prashant Sharma – Associate Professor – Department of
 Biomedical Engineering

Dr. Patrick van Rijn – Associate Professor – Department of Biomedical
 Engineering



university of
 groningen

Effect of impact energy on the formation of micro-cracks on healthy bovine cartilage.



Eleni Anna Kostopoulou

May 2023

INTERNSHIP REPORT

AUTHORED BY
ELENI ANNA KOSTOPOULOU

SUPERVISOR: DR. HUGO VAN DER VEEN

GRONINGEN, MAY 2023

1. FOREWORD

With great pleasure, I would like to present the following internship report titled "Effect of impact energy on the formation of micro-cracks on healthy and chondroitinase ABC digested bovine cartilage." This report reflects my experience and the skills I have acquired during my time as an intern at University Medical Center Groningen, where I worked on a research project that focused on the effect of impact energy on the formation of micro-cracks on bovine cartilage.

The goal of this report is to provide a detailed description of my experiences during the internship program, including the research methods, results, and conclusions. This research aims to create a more advanced experimental setup for future research, as well as to investigate the relationship between various impact energies, and the crack formation on bovine cartilage and their morphology and characteristics, using that setup.

I would like to express my gratitude to my mentors and colleagues who have supported me throughout my internship program. I would especially like to thank Dr. Hugo van der Veen, for his supervision, Dr. Prashant Sharma, for being my mentor through this entire process, as well as Dr. Ke Ren, for his valuable guidance and Hans Karper for his continuous help. Finally, I would like to thank my family and my friends for their continuous support.

I hope this report will be valuable for any researcher aiming to investigate the micro-crack initiation and formation due to impact and for anyone interested in cartilage biomechanics. Thank you for taking the time to read my report, and I welcome any feedback you may have.

2. SUMMARY

Osteoarthritis (OA) is a common joint disease that can lead to pain and dysfunction due to the deterioration of synovial joints and can cause reduced quality of life. Low-energy impacts on articular cartilage can initiate micro-cracks in the collagen network, which research has shown to be one of the earliest damaging alterations leading to OA.

The aim was, to create a cartilage-on-cartilage impact test, and to examine and determine the way impact energy affects the formation of these micro-cracks on healthy bovine cartilage.

To do so, the main idea was to place two bovine cartilage plugs, placed on top of each other, and drop on them a steel ball of known mass. By varying the dropping height of the ball, we were able to vary the impact energy applied on the cartilage surface. After the contact between the ball and the plug, the adsorbed energy was calculated by recording the rebound of the ball. After the micro-crack formation, their morphology was observed and analyzed using optical coherence tomography.

3. TABLE OF CONTENTS

1.	Foreword	1
2.	Summary	2
3.	Table of Contents	3
4.	List of Tables.....	4
5.	List of Figures	5
6.	Introduction	6
7.	Materials and Methods.....	7
7.1	Preparation of the Cartilage Plugs.....	7
7.2	Setup Preparation.....	8
7.3	Micro-Crack Formation with Varying Impact Energy.....	9
7.3.1	Impact test using steel ball with varying impact energy	9
7.3.2	Determination of collagen network orientation (Split lines)	10
7.3.3	Micro-crack morphology investigation using OCT.....	10
7.4	Statistical Analysis.....	10
8.	Results and Discussion	10
8.1	Micro-crack formation with varying impact energy	11
9.	Conclusion.....	13
10.	Bibliography	14

4. LIST OF TABLES

Table 1 Dropping heights and corresponding impact energies..... 9

5. LIST OF FIGURES

Figure 1 (a) Fresh bovine knee joint directly before the preparation of the cartilage plugs (b) Bovine knee joint after the flesh removal	7
Figure 2 Schematic illustration of the entire experimental process (a) Cartilage plugs are obtained from fresh bovine knee joints (b) Fixation of the cartilage plugs using a sponge case soaked in PBS buffer (c) The two plugs are placed under a drop tower that allows a steel ball to fall on the plugs ..	8
Figure 3 The two plugs are placed on top of each other, and a sponge cube surrounds them. Parafilm strips keep the whole structure together. Thin blue lines represent the PARAFILM strips ...	8
Figure 4 The falling and rebounding of the steel ball during the impact test	9
Figure 5 Captures of the steel ball reaching the surface of the plugs and the three rebounding heights H_2 , h_1 , h_2 , in the same time interval	10
Figure 6 Cartilage plugs after the impacting test with varying impact energy (a) Single micro-crack – 0.52603 J (b) Individual micro-cracks – 1.05205 J (c) Branched micro-cracks – 1.57808. Blue arrows indicate the split lines orientation	11
Figure 7 (a) The length of the cracks on the cartilage surface after the impact test (b) The endpoints of the cracks on the cartilage surface after the impact test.....	11
Figure 8 (a) The relation between the crack length on the cartilage surface after the impact test and the impact energy (b) The relation between the endpoints of the cracks on the cartilage surface after the impact test and the impact energy.....	11
Figure 9 TWOMPLI output for impact energy of 1.57808 J. The image name indicates the sample characteristics as Height_Upper/LowerPlug_NumberOfTest.png i.e., 180_U_A.png refers to 180 cm dropping height, upper plug and test A.....	12
Figure 10 Potential improved setup for impacting test.....	13

6. INTRODUCTION

Hyaline cartilage can be found on the end of the majority of bones [1] and its ECM consists of a highly dense collagen network [2]. The main collagen type is Type II, but small amounts of Types VI, IX, X and XI can also be found [1], among other components, such as water (75 wt%) [3], proteoglycans [2], and chondrocytes (<10 wt%) with low proliferation rate, which is the reason why cartilage is almost incapable to regenerate in case of lesion [3]. Additionally, there are no blood vessels or nerves found in cartilage [3]. Articular cartilage exists on the ends of bones in synovial joints [2] and it is a type of hyaline cartilage with a difference in the arrangement of the collagen fibers and the chondrocytes in the ECM [1]. Articular cartilage acts as the connective tissue of diarthrodial joints, and due to each organization and composition, it provides a smooth surface for the joints to slide, as well as load distribution with a low coefficient of friction [4]. The cartilage has distinctive zones with different collagen fibers alignment and functions. The thin superficial tangential zone is responsible for the shear, tensile, and compressive force resistance, and the fibers are tightly packed and parallel to the articular surface [4]. In the middle transitional, the fibers are organized obliquely, and this zone's function is the resistance to compressive forces [4]. The collagen fibrils in the deep zone are perpendicular to the articular surface, and they are anchored to the subchondral bone, through the calcified layer [4].

Osteoarthritis (OA) is a common joint disease that can lead to pain and dysfunction due to the deterioration of synovial joints [5] and can cause reduced quality of life [6]. Although various joint abnormalities and systemic diseases are associated with OA, it is still unknown how most of these cases are caused [5]. However, some risk factors for OA are age, joint injury, and excessive joint loading [5]. From the pathological aspect, OA involves the breakdown of cartilage, the abnormal modifying of subchondral bone, synovial inflammation, and degenerative changes in the meniscus or articular ligaments [6]. Low-energy impacts on articular cartilage can initiate micro-cracks in the collagen network, which research has shown to be one of the earliest damaging alterations leading to OA [7]. These micro-cracks are found in the calcified cartilage, subchondral plate, and metaphyseal trabecular network, and they seem to be the physical partings of the tissue matrix [6]. These micro-cracks can propagate during cyclic mechanical loads, further contributing to cartilage degeneration and the progression of OA [7]. However, the exact role of these micro-cracks in the initiation and progression of OA is still under investigation. The degree of micro-crack propagation during normal daily activities is not known. The knee joint is particularly vulnerable to injury, and injury to ligaments, tendons, cartilage, and bone within the knee can lead to post-traumatic OA. Micro-cracks in bone and surface fissures in cartilage have been extensively studied, however, recent research has shown that even low-energy impacts, that are considered non-injurious, can cause micrometer-scale micro-cracks in the collagen network [7].

As was mentioned above, the exact role of the micro-cracks caused by low-energy impacts is still unknown. Previous research has shown that an increase in impact energy leads to an increase in absorbed by the cartilage energy, as well as initiation of crack formation after the application of impact energy of 0.088 J [8]. However, during that research, a steel ball was directly impacting the cartilage, which is unrealistic and not close to real-life conditions. This research aims to (1) create a more advanced experimental setup for future research, as well as to (2) investigate the relation between various impact energies, and the crack formation on bovine cartilage and their morphology and characteristics, using that setup.

For the aims of the study, two cartilage plugs were made and placed on top of each other with their articular surface being in contact, mimicking the way cartilage surfaces interact with each other in the synovial joints. The cartilage plugs were placed under a cylinder, allowing a steel ball of known mass to drop on them. In addition, a custom-made sponge case surrounded the two plugs and kept them hydrated with the use of phosphate-buffered saline. We used the setup described above, and dropped the steel ball from various heights, altering this way the impact energy. After the impact, the rebound of the ball was recorded in order to calculate the absorbed by the cartilage energy, as well as the residual in the ball energy. The plugs were later observed under optical coherence tomography (OCT), to determine the morphology of the formed micro-cracks, and relate their characteristics with the impact energy.

7. MATERIALS AND METHODS

7.1 PREPARATION OF THE CARTILAGE PLUGS

The cartilage plugs were obtained from fresh bovine knee joints (**Fig. 1a**) (approximately two-year-old bulls), that were purchased from a slaughterhouse in Groningen (Kroon Vlees, Groningen, the Netherlands). The knee joints were transferred to University Medical Center Groningen and the plugs were made on the same day. The whole process was done at room temperature (20-24 °C). Firstly, the flesh was carefully removed from the joint, with the use of a scalpel, avoiding touching the cartilage surface (**Fig. 1b**). The top parts of both femoral condyles were cut off, using an electric multitool (Fein, Stuttgart, Germany). With the use of an electric hollow drill, cartilage plugs with a diameter of 12 mm and a length of approximately 10 mm were drilled from the center part of the femoral condyles (**Fig. 2a**). During the entire preparation process, the cartilage surface was constantly wetted with PBS buffer, and till further process, all the samples were kept in PBS buffer at 4 °C. From each bovine, six to eight cartilage plugs could be obtained.

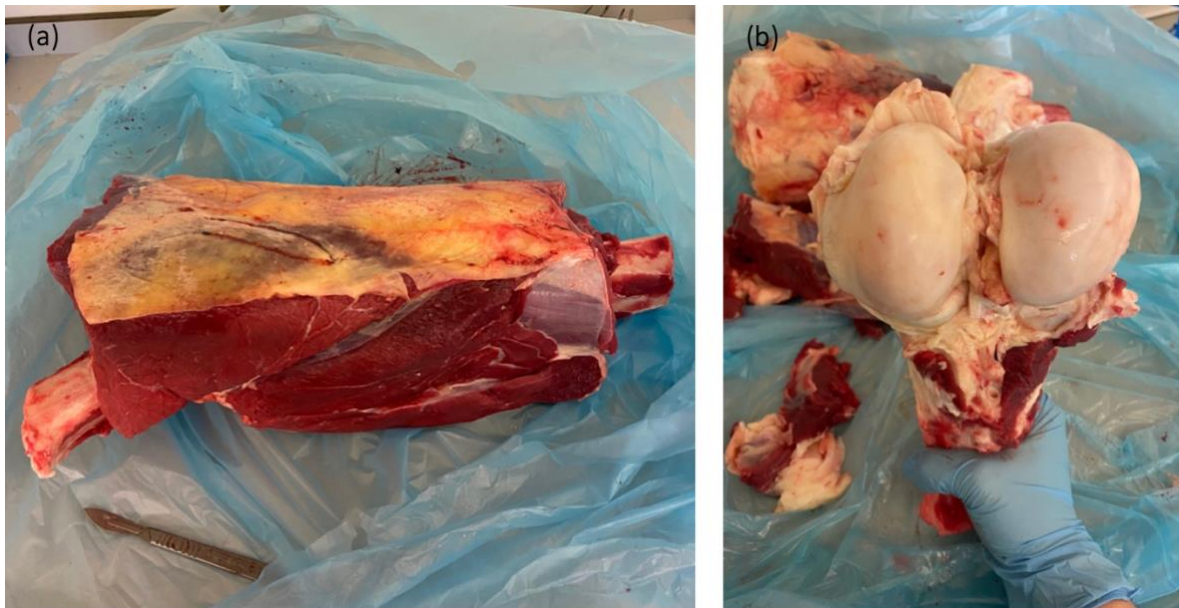


Figure 1 (a) Fresh bovine knee joint directly before the preparation of the cartilage plugs (b) Bovine knee joint after the flesh removal

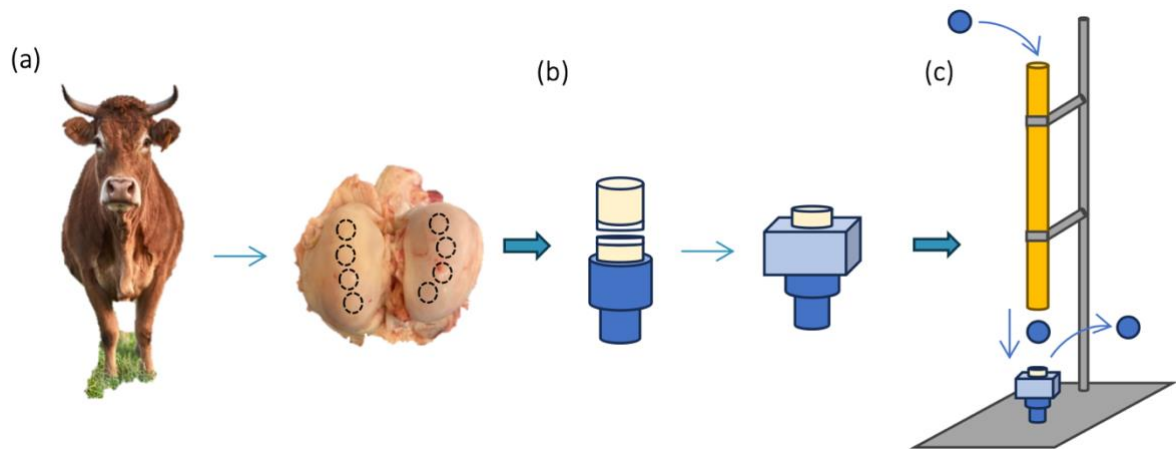


Figure 2 Schematic illustration of the entire experimental process (a) Cartilage plugs are obtained from fresh bovine knee joints (b) Fixation of the cartilage plugs using a sponge case soaked in PBS buffer (c) The two plugs are placed under a drop tower that allows a steel ball to fall on the plugs

7.2 SETUP PREPARATION

After the preparation of the plugs, one of them was placed in a steel base, that would keep it stable (**Fig. 2b**). The second cartilage plug was placed on top of it, and it was fixated using a case made from a highly absorbent sponge. The sponge was cut into cubes, and then using the same drill that was used for the plug preparation, holes were cut into the cubes, so the plugs would perfectly fit. The sponge was soaked in PBS buffer, providing constant hydration and lubrication between the two cartilage surfaces. Finally, narrow strips of PARAFILM were used to keep the entire structure together, over the sponge (**Fig. 3**).



Figure 3 The two plugs are placed on top of each other, and a sponge cube surrounds them. Parafilm strips keep the whole structure together. Thin blue lines represent the PARAFILM strips

7.3 MICRO-CRACK FORMATION WITH VARYING IMPACT ENERGY

7.3.1 Impact test using steel ball with varying impact energy

For the impact test, a drop tower was used (**Fig. 2c**). The two plugs were placed under the drop tower, which allowed a steel ball to fall on them. The steel ball weighed 0.090 kg and it had a diameter of 20 mm, and it was used as the impactor. By varying the dropping height (H_1), we were able to vary to impact energy (E_i) applied to the plugs, which equals the gravitational potential energy of the steel ball falling on the cartilage plugs from a specific height (H_1). To capture the steel ball's fall and

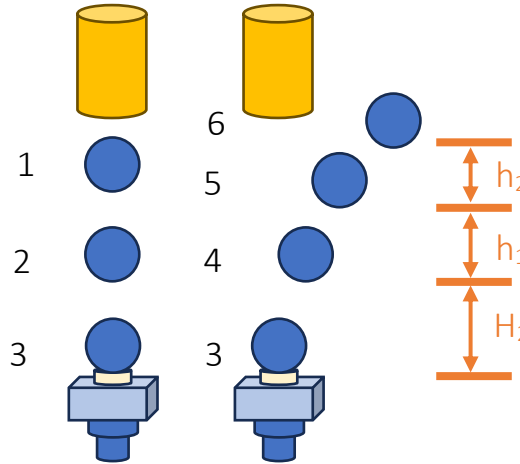


Figure 4 The falling and rebounding of the steel ball during the impact test

rebound, a camera was used (iPhone 11, Apple Inc., USA) (**Fig. 5**), in slow motion mode. After the recording of the ball motion, the following formulas were used to calculate the absorbed by the cartilage energy (E_a), by using the rebounding heights H_2 , h_1 , and h_2 (**Fig. 4**), in the same time interval (t).

$$E_i = mgH_1 \quad (1)$$

$$E_i = \frac{1}{2}mv_1^2 + mgH_2 + E_a \quad (2)$$

$$h_1 + h_2 = v_1(2t) - \frac{1}{2}g(2t)^2 \quad (3)$$

Where m is the mass of the steel ball, g is the gravitational constant, v_1 is the velocity at rebounding height h_1 and t is the time interval.

For the impacting test, we chose the dropping heights H_1 shown in Table 1 and the corresponding impact energy E_i .

Table 1 Dropping heights and corresponding impact energies

Dropping Height (H_1)	60 cm	80 cm	100 cm	120 cm	150 cm	160 cm	180 cm
Impact Energy (E_i)	0,52603 J	0,70137 J	0,87671 J	1,05205 J	1,31507 J	1,40274 J	1,57808 J

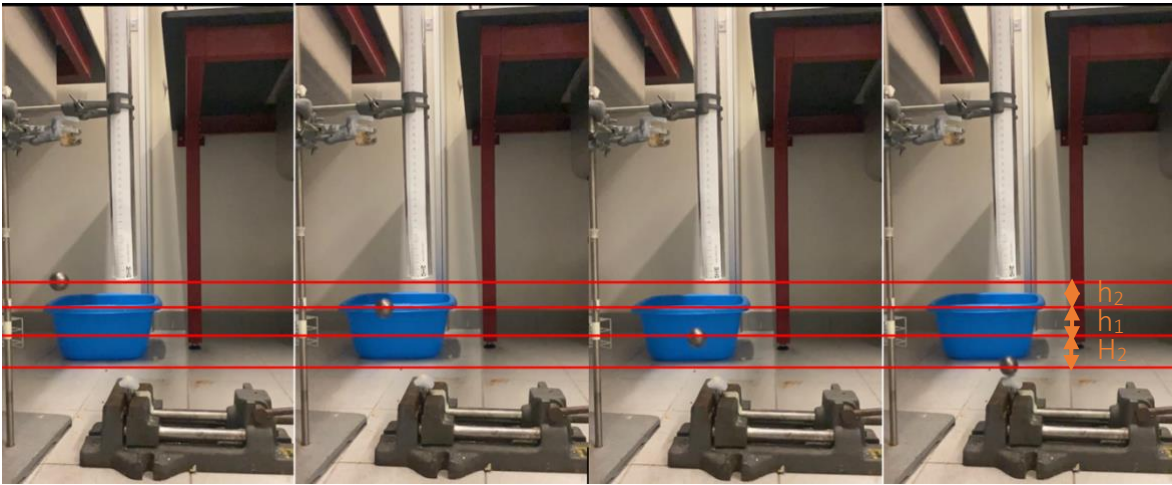


Figure 5 Captures of the steel ball reaching the surface of the plugs and the three rebounding heights H_2 , h_1 , h_2 , in the same time interval

7.3.2 Determination of collagen network orientation (Split lines)

To determine the orientation of the fibers in the collagen network a dissecting needle was used, by inserting it in the cartilage surface to the level of the subchondral bone at a 90° angle, at the edge of the plug. The needle was first dipped in Indian ink (Winsor & Newton, London, United Kingdom), to stain the cartilage matrix. The insertion of the needle causes the collagen fibers of the superficial layer of the cartilage to split, and the Indian ink made that split visible.

7.3.3 Micro-crack morphology investigation using OCT

The surface of the cartilage plugs was covered with the same Indian ink, used for the determination of the collagen network orientation. The ink penetrated the micro-cracks and made them visible. Afterward, the plugs were washed with PBS buffer, to remove the excess ink from the cartilage surface, and they were placed immediately after under the OCT Ganymede II device (Thorlabs Gany-mede, Newton, NJ, USA) with a 930 nm center wavelength white light beam through a Thorlabs LSM03 objective scan lens, for the observation of the crack morphology. The dimensions of the scanned area were $6 \times 6 \times 2 \text{ mm}^3$. The horizontal (x-y) size of the image was 1000 pixels x 1000 pixels, and the vertical (z) size of the image was 1000 pixels. The images of the cartilage surface were exported using the OCT software (ThorImage OCT 4.1). To assess the length and endpoints of the formatted cracks, the TWOMBLLI plugin for FIJI Image, was used (**Fig. 9**).

7.4 STATISTICAL ANALYSIS

The process of the data was done using GraphPad Prism 9 (GraphPad Software, La Jolla California USA), and they were expressed as means \pm SD. Three independent but identical experiments were performed for each height, therefore each impact energy.

8. RESULTS AND DISCUSSION

8.1 MICRO-CRACK FORMATION WITH VARYING IMPACT ENERGY

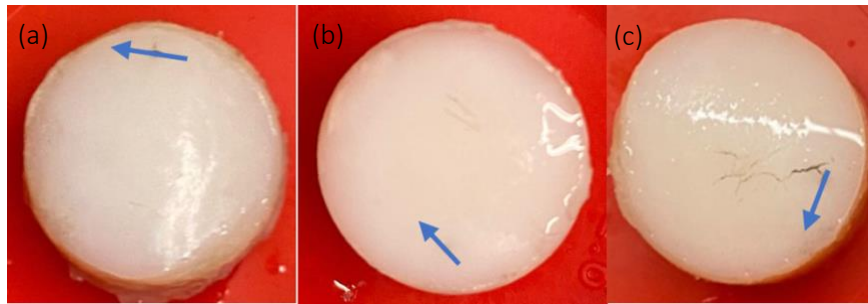


Figure 6 Cartilage plugs after the impacting test with varying impact energy (a) Single micro-crack – 0.52603 J (b) Individual micro-cracks – 1.05205 J (c) Branched micro-cracks – 1.57808. Blue arrows indicate the split lines orientation

Fig. 4a & b show the length, as well as the number of endpoints, of the cracks on the cartilage surface, as a function of impact energy, whereas Fig. 5a & b show the absorbed by the cartilage plugs energy and the residual in the steel ball energy, as a function of impact energy. Both the total crack length and the total number of endpoints did not seem to differ significantly at low-impact energy but appeared to increase progressively at higher-impact energy. At the lowest impact energy of 0.526 J, the total crack length was around 2.087 ± 3.615 mm (**Fig. 7a**) with an average number of 2.000 ± 3.464 endpoints (**Fig. 7b**). The significant increase in both values was observed at the impact energy of 1.315 J, at which the total crack length was equal to around 7.220 ± 4.443 mm (**Fig. 7a**) and the endpoints were 8.000 ± 4.000 (**Fig. 7b**). At this energy, the cracks arising had branches (spread cracks), whereas, before that point, only single or individual cracks were observed. After that critical impact

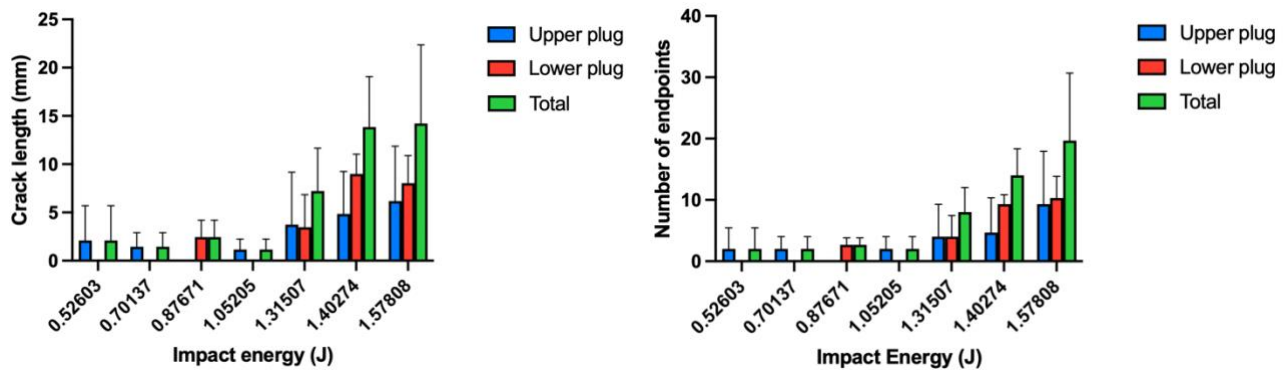


Figure 8 (a) The relation between the crack length on the cartilage surface after the impact test and the impact energy (b) The relation between the endpoints of the cracks on the cartilage surface after the impact test and the impact energy

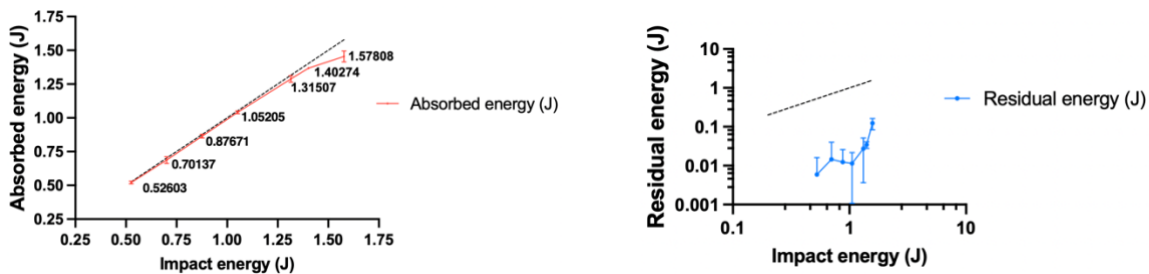


Figure 7 (a) The length of the cracks on the cartilage surface after the impact test (b) The endpoints of the cracks on the cartilage surface after the impact test

energy (1.315 J), the length of the cracks formatting on the cartilage surface, and their endpoints, increase for both the lower and the upper plugs, with no significant difference.

Regarding the energy absorbed by the cartilage plugs, it was increased almost linearly, till the impact energy was equal to 1.315 J, meaning that all or almost all the impact energy was absorbed by the cartilage plugs. At the impact energy of 0.526 J, the cartilage plugs absorbed energy equal to 0.520 ± 0.010 J (Fig. 8a), and the energy that remained in the steel ball after the rebound was equal to 0.006 ± 0.010 J (Fig. 8b). At the critical impact energy of 1.315 J, where the significant increase in the crack length and the number of endpoints were observed, the absorbed energy was equal to 1.288 ± 0.024 J (Fig. 8a), whereas the residual energy was almost 0.028 ± 0.024 J (Fig. 8b). At energy higher than 1.315 J, there is a deviation from the linear behaviour, meaning that there is an increase in the energy remaining in the steel ball.

After the impacting test, the orientation of the collagen fiber network was determined, in order to be compared with the orientation of the micro-cracks and to determine whether there is a relation between the two (Fig. 6). The angles formed between the individual cracks ranged from 0° to 90° , but no strict relation was observed. However, these angles indicate the location of the disruption on the collagen fiber network. According to Gelse et al, if the angle is 0° , it means that the damage occurred between the cross-links, whereas if the angle is 45° or 90° , the disruption occurred in the cross-links and the collagen Type II.

	A	B	C
1	Image	Total Length	Endpoints
2	180_U_A.png	7,347	11
3	180_L_A.png	10,444	14
4	180_U_B.png	11,199	17
5	180_L_B.png	8,754	10
6	180_U_C.png	0	0
7	180_L_C.png	4,896	7

Figure 9 TWOMPLI output for impact energy of 1.57808 J. The image name indicates the sample characteristics as Height_Upper/LowerPlug_NumberOfTest.png i.e., 180_U_A.png refers to 180 cm dropping height, upper plug and test A

As mentioned before, the aim of the research was to create a cartilage-on-cartilage experimental setup, in contrast to the previously used setup, where the impacting test would be performed with the steel ball impacting directly the cartilage surface. This research confirmed the findings of the previous research, specifically that increase in the impact energy causes increase in crack length and number of endpoints, as well as increase in the absorbed and residual energy. However, the results of our research indicate that the impact energy required for the formation of micro-crack formation is higher. The same impact energy caused the formation of longer micro-cracks with more endpoints when the steel ball impacted directly the cartilage surface. For impact energy of 0.701 J, the previous research showed that cracks with around 12.000 ± 15.000 mm length and around 10.000 ± 10.000 endpoints were formatted, whereas in our experiments, the same impact energy caused the formation of 1.457 ± 1.450 mm long micro-cracks, with 2.000 ± 2.000 endpoints. Also, our research showed that the impact energy required for the formation of branched micro-cracks, instead of single or individual cracks was 1.315 J, in comparison to the previous research, which showed that the energy required for the same action was 0.526 J. Additionally, in the case of two plugs, for impact energies lower than 1.315 J, all or almost all the impact energy was absorbed but the plugs, which was not observed in the case of one plug, where regardless the impact energy, most of that energy

was absorbed by the plugs, but approximately 25-30% of the impact energy remained in the steel ball, causing it to rebound.

9. CONCLUSION

Increase in impact energy leads to increase in the absorbed by the cartilage plugs energy, and for impact energy lower than 1.315 J, almost all energy is absorbed by the cartilage plugs. For energy higher than 1.315 J a significant increase in the length and the number of endpoints of the micro-cracks was observed, which kept increasing progressively. Additionally, the cracks formatted due to impact energy higher than 1.315 J, appeared to be branched, instead of single or individual.

The setup created for the impacting test seemed to work sufficiently, however, there are potential alternatives that could improve the experimental process, as well as suggestions for future experiments. Firstly, an improved setup would include one of the cartilage plugs as the impactor, instead of the steel ball. This setup could use a spring, with known spring constant (k), where one of the plugs is fixated on the end of it, and by compressing and releasing the spring, the impact energy could be defined, based on the elastic potential energy (PE) (Fig. 10).

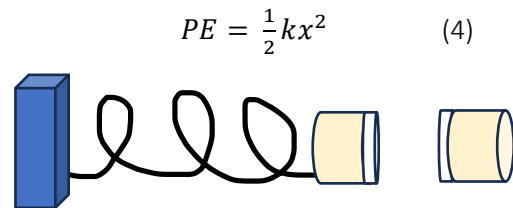


Figure 10 Potential improved setup for impacting test

Secondly, OCT images could be taken before the impacting test too, to determine whether there are pre-existing micro-cracks or other irregularities on the cartilage surface, so the plugs can be rejected.

In addition, instead of PBS, synovial fluid or other non-Newtonian fluid with characteristics similar to the synovial fluid, could be used between the two plugs, to mimic better the real-life conditions. Finally, regarding the realistic conditions, the use of one concave and one convex surface, instead of two convex cartilage surfaces, could also help.

As for future research, it would be sound to repeat the experiments for energies ranging from 1.052 J to 1.315 J, to determine the exact energy required for the formation of branched micro-cracks, as well as the exact point the length and the endpoints of the micro-cracks start increasing. Lastly, the experiments should be repeated, for enzymatically degraded plugs, as OA is caused by the simultaneous enzymatic degradation and micro-crack formation on the cartilage surface, and the results should be compared with the results of the previous and current research.

10. BIBLIOGRAPHY

- [1] R. L. Maynard and N. Downes, "Introduction to the Skeleton: Bone, Cartilage and Joints," in *Anatomy and Histology of the Laboratory Rat in Toxicology and Biomedical Research*, Elsevier, 2019, pp. 11-22.
- [2] J. Watkins, "Biomechanics of Musculoskeletal Adaptation," in *Comprehensive Biomedical Physics*, Elsevier, 2014, pp. 1-37.
- [3] A. J. Salgado, J. M. Oliveira, A. Martins, F. G. Teixeira, N. A. Silva, N. M. Neves, N. Sousa and R. L. Reis, "Tissue Engineering and Regenerative Medicine: Past, Present, and Future," *International Review of Neurobiology*, vol. 108, pp. 1-33, 2013.
- [4] A. J. S. Fox, A. Bedi and S. A. Rodeo, "The Basic Science of Articular Cartilage: Structure, Composition, and Function," *Sports health*, vol. 1, no. 6, p. 461–468, 2009.
- [5] J. A. Buckwalter, D. D. Anderson, T. D. Brown, Y. Tochigi and J. A. Martin, "The Roles of Mechanical Stresses in the Pathogenesis of Osteoarthritis," *Cartilage*, vol. 4, no. 4, p. 286–294, 2013.
- [6] A. Kaspiris, E. Chronopoulos, E. Vasiliadis, L. Khaldi, D. Melissaridou, I. Iliopoulos and O. Savvidou, "Sex, but not age and bone mass index positively impact on the development of osteochondral micro-defects and the accompanying cellular alterations during osteoarthritis progression," *Chronic Diseases and Translational Medicine*, vol. 8, no. 1, pp. 41-50, 2022.
- [7] S. Santos, N. Emery, C. Neu and D. Pierce, "Propagation of microcracks in collagen networks of cartilage under mechanical loads," *Osteoarthritis and Cartilage*, vol. 27, no. 9, pp. 1392-1402, 2019.
- [8] K. Ren, "Chondral surface cracking due to mechanical impact and its influence in lubrication [Unpublished Article]," 2022.